# Advances in Geo-Energy Research

### Original article

## Microscale interaction mechanism between shale oil and CO<sub>2</sub> in mixed wettability nanopores

Fengjiao Wang<sup>1</sup>, Xianghao Meng<sup>1</sup>, He Xu<sup>1</sup>, Yipu Liang<sup>2</sup>, Yikun Liu<sup>1,3</sup>\*

#### **Keywords:**

Shale oil mixed wettability nano-confinement effect microscopic interaction molecular dynamics

#### Cited as:

Wang, F., Meng, X., Xu, H., Liang, Y., Liu, Y. Microscale interaction mechanism between shale oil and CO<sub>2</sub> in mixed wettability nanopores. Advances in Geo-Energy Research, 2025, 18(3): 231-241.

https://doi.org/10.46690/ager.2025.12.03

#### **Abstract:**

Microscale interactions are pronounced in shale nanopores, while the relevant mechanisms between multiphase fluids remain unclear at present. In this paper, the CO<sub>2</sub> displacement process in shale porous media with mixed wettability is simulated, with the aim to reveal the microscopic interphase mechanisms and assess CO2 displacement efficiency and storage performance. The results indicate that in the initial state, under the predominant effect of van der Waals forces, oil molecules are present in adsorbed and free states, while water molecules exist as films and clusters in the three types of channels, driven by the combined action of van der Waals forces, Coulomb forces and hydrogen bonds. During the displacement process, CO<sub>2</sub> preferentially enters hydrophilic channels, followed by mixed-wetting channels, and finally lipophilic channels. Instantaneous dipole moments between non-polar molecules make van der Waals forces the dominant factor in mutual miscibility. The permanent dipole of polar molecules and the induced dipole of nonpolar molecules synergistically enhance the contribution of Coulomb force during the competitive adsorption process. However, the presence of "water bridge" within mixedwetting channels significantly inhibits CO<sub>2</sub> penetration and impairs oil stripping. The final displacement efficiency and storage efficiency are 43.08% and 5.99%, respectively, both significantly lower than those in hydrophilic and lipophilic channels. This study clarifies the microscale interaction mechanisms in shale reservoirs with mixed wettability, offering practical guidance for effective shale reservoir exploitation.

#### 1. Introduction

As traditional oil reserves are gradually exhausted, unconventional resources, typified by shale oil, have emerged as a global research hotspot (Chico et al., 2023). However, single-well production rate in shale reservoirs declines rapidly, and the recovery rate under depletion development is extremely low (Alsubaih et al., 2025). Against this backdrop, CO<sub>2</sub>, as an excellent displacing medium, has shown great application potential in the domain of shale oil exploitation (Liu et al., 2024; Wang et al., 2025). It can not only effectively

reduce interfacial tension and facilitate oil-CO<sub>2</sub> miscibility owing to its high solubility but also engage in competitive adsorption with shale oil on the reservoir surface, stripping and replacing oil molecules adsorbed on the surface to realize the double benefits of enhanced oil recovery and geological storage (Zhang et al., 2023; Chen et al., 2024).

As typical nano-confined spaces, shale reservoirs have a widely developed micro-nanopore structure within them, which leads to a complex interphase microscopic interaction mechanism during the process of CO<sub>2</sub> displacement and

Yandy Scientific Press

 $^* Corresponding \ author.$ 

E-mail address: wangfengjiao@nepu.edu.cn (F. Wang); m18348579840@163.com (X. Meng); xuhe19990909@163.com (H. Xu); yxl6331@psu.edu (Y. Liang); liuyikun@nepu.edu.cn (Y. Liu).

2207-9963 © The Author(s) 2025.

Received October 1, 2025; revised October 27, 2025; accepted November 13, 2025; available online November 16, 2025.

<sup>&</sup>lt;sup>1</sup>Key Laboratory for Enhanced Oil & Gas Recovery of the Ministry of Education, Northeast Petroleum University, Daqing 163318, P. R. China

<sup>&</sup>lt;sup>2</sup>Department of Energy and Mineral Engineering, The Pennsylvania State University, University Park, PA 16802, USA

<sup>&</sup>lt;sup>3</sup>Sanya Offshore Oil and Gas Research Institute, Northeast Petroleum University, Sanya 572024, P. R. China

storage (Ho and Wang, 2019; Mohammed and Gadikota, 2019; Goral et al., 2020). Especially, the pore size of shale is closer to the molecular scale, and the interphase microscopic forces will be significantly enhanced within the nanoscale confined space due to the reduced intermolecular distance (Cui et al., 2022; Wang et al., 2023). Therefore, clarifying the microscopic interaction mechanism among multiphase fluids within shale reservoirs is conducive to the efficient development and utilization of oil. At present, research on the microscale mechanism mainly adopts experimental and simulation methods. Experimental methods (such as AFM and SEM) can achieve nanoscale observation, but they struggle to capture real-time dynamic interaction processes. In contrast, the molecular dynamics simulation method overcomes the limitations of experimental techniques and visually reproduces the adsorption and migration processes of fluids within nanochannels at the molecular scale, thus becoming an important tool for studying micro-interaction mechanisms (Cai et al., 2024; Hong et al., 2024; Lappala, 2024). Previous studies using molecular dynamics methods to construct shale oil-CO<sub>2</sub> component models found that van der Waals forces and Coulomb forces are the two primary microscopic interaction forces (Masoud et al., 2023; Wang et al., 2025b). Nonpolar molecules are affected by van der Waals forces, while Coulomb forces mainly act between polar molecules with a fixed charge distribution. The combined effect of the two types of microscopic intermolecular forces significantly affects the adsorption and diffusion behaviors of fluid molecules within pore throats with varying wettability (Nguyen et al., 2017; Babaei et al., 2023; Shi et al., 2023).

To further clarify the influence of the microscopic interaction mechanism between multiphase components on the occurrence and migration laws of fluids within the channels, Wang et al. constructed surface models with different wettability based on molecular dynamics methods and compared the adsorption behaviors of surfaces with different wettability (Wang et al., 2022; Sanchouli et al., 2024; Wan et al., 2024). Research has found that the strong Coulomb interaction of polar minerals within the channels exhibits obvious hydrophilicity, while the strong van der Waals interaction between non-polar minerals exhibits lipophilicity. The stronger the non-polar interaction on the pore surface is, the better the lipophilicity effect, and the greater the number of shale oil molecules are adsorbed on the pore surface, the thicker the adsorption layer. Some scholars further constructed CO2 displacement models within channels with different wettability, and the results showed that on account of the intense intermolecular interaction between lipophilic surface and oil molecules, shale oil molecules would form a tight adsorption layer inside the channel. CO<sub>2</sub> could hardly detach the adsorbed oil molecules and tended to diffuse along the central region of the channels, resulting in a poor peeling effect (Sedghi et al., 2016; Perez and Devegowda, 2020). However, the interaction between CO<sub>2</sub> and the hydrophilic surface is strong. CO2 is more likely to diffuse near the pore surface, and the displacement effect of shale oil is better (Dong et al., 2023b; Wu et al., 2024; Zhao et al., 2024). At present, the micro-mechanisms of interaction among multiphase fluids during the process of CO<sub>2</sub> displacement has primarily focused on single wettability pore models, whereas real shale reservoirs exhibit distinct mixed-wettability characteristics. Studies on how the mixed-wettability properties of shale itself influence interphase van der Waals forces, Coulomb forces, and other microscopic mechanisms remain scarce.

To address the above shortcomings, this study establishes a parallel channel system of shale with mixed-wetting based on molecular dynamics (MD) simulation, and elucidates the microscopic mechanisms between phases under mixed-wettability and nanoscale confinement effects. Firstly, the occurrence characteristics of the fluid in the mixed-wetting system are revealed from the perspective of microscopic interactions such as van der Waals forces, Coulomb force, and hydrogen bonds. Subsequently, the interphase microscopic interaction during the CO<sub>2</sub> displacement process is clarified, and the contribution ratios of the two non-bonded interaction energies are determined. Finally, the CO<sub>2</sub> displacement and storage efficiencies are evaluated.

#### 2. Models and methods

#### 2.1 Model construction

In order to clarify the interphase microscopic mechanisms of shale with mixed wettability and nano-confinement effects, quartz minerals, which are common in reservoirs, were selected to establish a model of a mixed wettability system (containing hydrophilic channels, lipophilic channels and mixed-wetting channels) (Zhao et al., 2017). To characterize surfaces with different wettability, the hydroxyl and methyl groups were proportionally arranged on the quartz surface. The dimensions of each wall were 24.55 and 102.05 Å, respectively, and the width of the channels were set to 40 Å. C<sub>12</sub>H<sub>26</sub> molecules and water molecules were placed inside the nano-channel. During the model construction process, in order to fully compare the interphase microscale interaction mechanism, it is necessary to ensure the consistency of other conditions. Therefore, we chose to fill the shale oil and water components into each pore with different wettability in a typical water-oil-water configuration, followed by a prolonged relaxation process, to fully restore the distribution state of the components under realistic reservoir conditions. The internal pressure of each channel was maintained at 20 MPa, and the CO<sub>2</sub> system was added to form an initial system model, as shown in Fig. 1. The number of molecules in the initial model is showen in Table 1.

#### 2.2 Simulation methods

In this paper, LAMMPS software was employed to perform MD simulations, while visual molecular dynamics software was utilized for the visualization of molecular trajectories (Humphrey et al., 1996; Thompson et al., 2022). The SPC/E model was used to model water molecules, the EPM2 force field was used to describe CO<sub>2</sub> molecules, and the quartz crystal and the hydroxylated quartz surface were modeled with the parameter of the ClayFF force field (Bao et al., 2025). The OPLS-AA force field was employed to describe the alkane and the methyl quartz surface (William et al., 1996). The specific

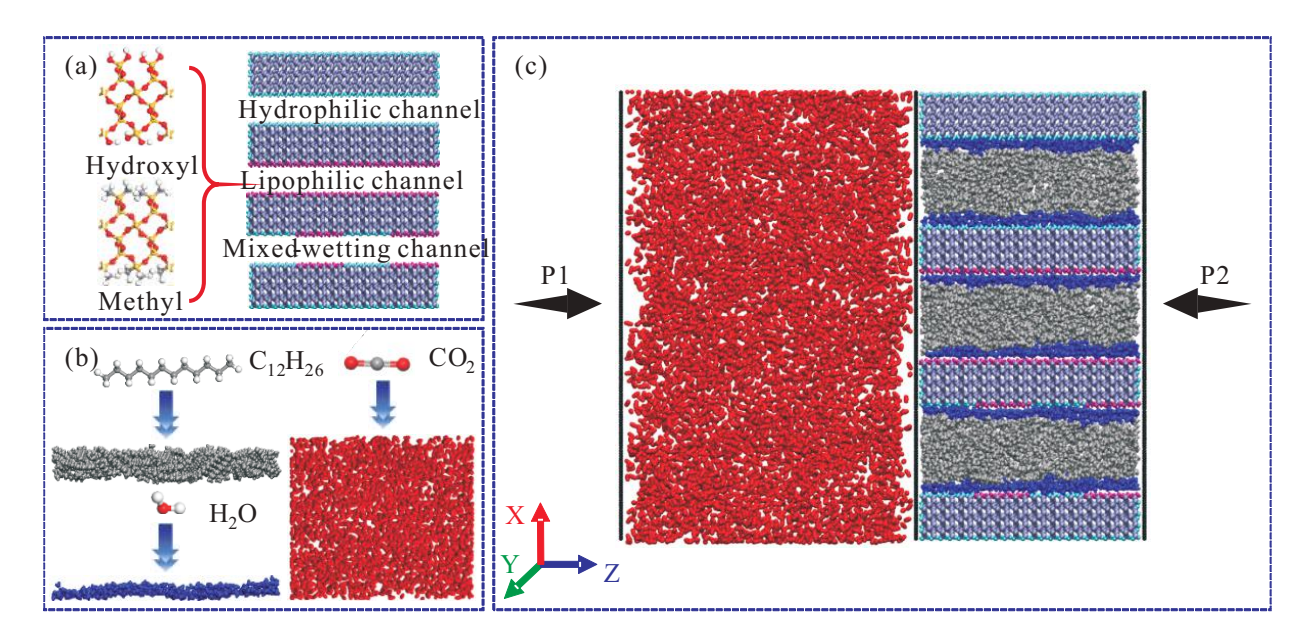


Fig. 1. (a) Surfaces with different wettability, (b) fluid component model and (c) mixed wettability system of shale.

**Table 1**. Number of C<sub>12</sub>H<sub>26</sub> and water molecules inside the displacement model.

Overall system	Hydrophilic channel		Lipophilic channel		Mixed-wetting channel	
CO <sub>2</sub>	$C_{12}H_{26}$	Water	$C_{12}H_{26}$	Water	$C_{12}H_{26}$	Water
7,000	176	800	176	800	176	800

force field parameters are shown in Table 2. Periodic boundary conditions were used for all simulations, and the time step was set to 1 fs. In addition, long-range electrostatic interactions were described using the Coulomb potential, with the 10 Å cutoff radius, and the non-bond interactions followed the Lennard-Jones potential. For different atom types, the Lorentz-Berthelot combining rules govern their mutual interactions according to the following formula (Jiang et al., 2024):

$$E_{ij} = \frac{q_i q_j}{4\pi \varepsilon_0 r_{ij}} \tag{1}$$

$$E_{ij} = \frac{q_i q_j}{4\pi \varepsilon_0 r_{ij}}$$

$$U_{ij} = 4\varepsilon_{ij} \left[ \left( \frac{\sigma_{ij}}{r_{ij}} \right)^{12} - \left( \frac{\sigma_{ij}}{r_{ij}} \right)^6 \right]$$
(2)

$$\varepsilon_{ij} = \sqrt{\varepsilon_i \varepsilon_j} \tag{3}$$

$$\sigma_{ij} = \frac{\sigma_i + \sigma_j}{2} \tag{4}$$

where  $E_{ij}$  represents the coulombic interaction, kcal/mol;  $q_i$ ,  $q_j$  represent the atomic charge of i and j, respectively, e;  $\varepsilon_0$ is the dielectric constant of a vacuum, F/m;  $r_{ij}$  represents the distance of i and j, Å;  $U_{ij}$  represents the van der Waals interaction, kcal/mol;  $\varepsilon_{ij}$  represents the Lennard-Jones well depth between i and j, J;  $\varepsilon_i$  represents the well depth of atom i, J;  $\varepsilon_i$  represents the well depth of atom j, J;  $\sigma_{ij}$  represents the zero-potential distance between atom i and j, Å;  $\sigma_i$  represents the zero-potential distance of atom i, Å;  $\sigma_i$  represents the zeropotential distance of atom i, Å.

In order to stabilize the distribution of each component in the pore, firstly, a conjugate gradient algorithm was used to

achieve stable initial configuration by continuously adjusting the atomic positions. The MD was conducted using the canonical ensemble under constant particle number, volume, and temperature conditions. Subsequently, the pressure difference method was used to carry out the displacement process. Rigid He plates were positioned on both sides of the system, and the plates were configured to move solely along the Z axis. External forces P1 (0.4 MPa/Å) and P2 (0.2 MPa/Å) were applied to plates according to the conversion relationship in (Zhan et al., 2020):

$$f = \frac{\nabla P L_z A}{N} \times 1.43885 \times 10^{-4} \tag{5}$$

where f represents the external force, kcal/(mol·Å);  $\nabla p$  represents the pressure gradient, MPa/Å;  $L_z$  represents the length along the flow direction, A; A represents the area of the nanopore,  $Å^2$ ; N represents the total atomic count in the nanopore.

#### 2.3 Model validation

#### 2.3.1 Density

The appropriate selection of force field parameters serves as a critical factor in guaranteeing the accuracy of simulation outcomes. To validate the reliability of the force fields before the formal simulation, common alkane molecule force field (OPLS-AA, TraPPE-UA, NIST) and water molecular force field (SPC, SPC/E, TIP4P, NIST) were chosen for comparative analysis. The initial system was assigned different force field

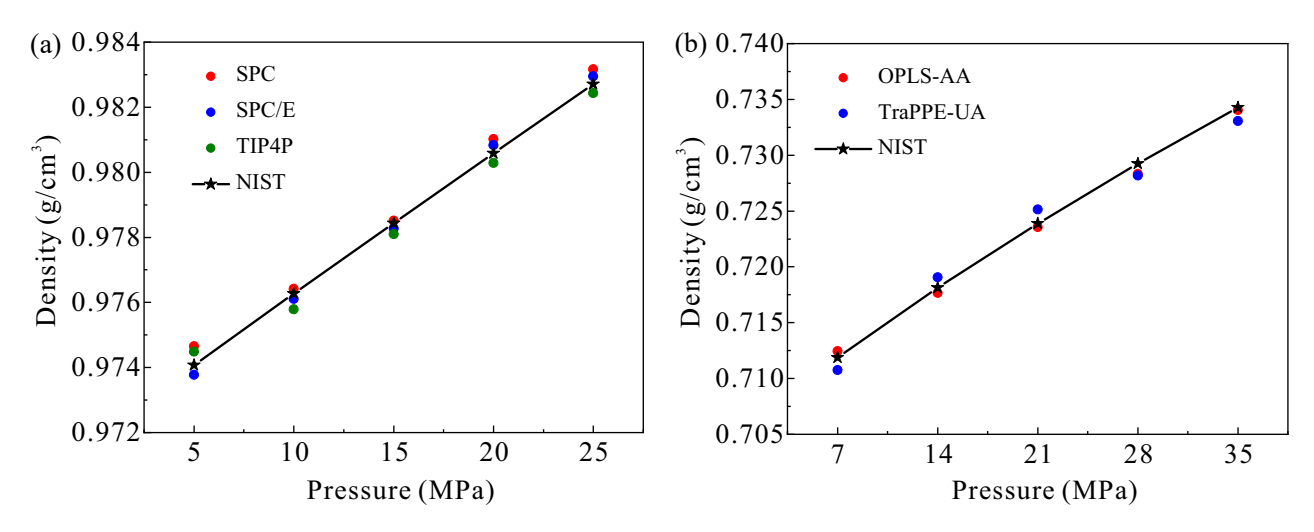


Fig. 2. Verification of force field for (a) water and (b) alkane molecule.

**Table 2.** Force field parameter for alkane, water, CO<sub>2</sub>, and quartz.

Atom types	$\varepsilon_0$ (kcal/mol)	$\sigma_{ij}$ (Å)	q (e)
C (alkane, CH <sub>3</sub> <sup>-</sup> )	0.066	3.5	-0.18
C (alkane, CH <sub>2</sub> <sup>-</sup> )	0.066	3.5	-0.12
H (alkane, H-C)	0.03	2.5	0.06
O (water, O-H)	0.1554	3.1655	-0.82
H (water, H-O)	0	0	0.41
$C (CO_2, C=O)$	0.0559	2.757	0.6512
$O(CO_2, C=O)$	0.1599	3.033	-0.3256
Si (quartz, Si-O)	$1.8405 \times 10^{-6}$	3.30203	2.1
O (quartz, O-Si)	0.1554	3.16556	-1.05
O (quartz, O-H)	0.1554	3.16556	-0.95
H (quartz, H-O)	0	0	0.425
C (quartz, Si-C)	0.066	3.50	-0.18
H (quartz, C-H)	0.03	2.42	0.06

parameters and the bulk density of the fluid under different pressure conditions was measured under the NPT ensemble. The results of molecular dynamics simulation were compared with those published by NIST, as shown in Fig. 2. The force field selected both matched the experimental values well.

#### 2.3.2 Contact angle

To further validate the accuracy of the force field and the initial model, the equilibrium molecular dynamics simulation of the mixed-wetting system was conducted, as shown in Fig. 3. The mixed wettability of shale and the nano-confinement effects make the oil exist in the forms of adsorption phase (peak curve region) and free phase (straight line region). Water exists as clusters in the lipophilic and mixed-wetting channels, and the average value of three-phase contact angles is 116.6° and 55.75°, respectively. The three-phase contact

angles formed in channels with different wettability align with the actual wall wettability (Xu et al., 2024; Wang et al., 2025a), indicating that this simulation has high credibility.

#### 3. Results and discussion

#### 3.1 Displacement process of CO<sub>2</sub>

The occurrence characteristics of fluids and the CO<sub>2</sub> displacement process under mixed wettability and nanoconfinement effects are shown in Figs. 3 and 4, respectively. Since the hydroxyl groups are polar molecules when modified on both the hydrophilic surface and water, the water molecules adsorb adjacent to the surface as a water film, while oil fills the remaining volume of the hydrophilic channel. The interaction between the permanent dipole moments of these polar molecules results in a significant Coulomb force between water and the hydrophilic channel, attracting water molecules to the pore wall and promoting the further formation of hydrogen bonding with surface hydroxyl groups. To further illustrate the microscopic interaction forces among components, the non-bonding interaction between different wettability surfaces and liquid, the hydrogen bonds between water-water and the water-surface were further statistically analyzed. Among them, hydrogen bonds are formed by covalent bonding between hydrogen atoms and atoms with high electronegativity. A hydrogen bond is deemed to form between the donor and acceptor atom if the distance between them is less than the distance cutoff (3.0 Å) and the angle falls within the angle cutoff (30°) (Janamejaya and Ladanyi, 2009). The non-bonding energy and hydrogen bonding between components are shown in Fig. 5. Under the combined effect of Coulomb forces and hydrogen bonds, water is stably adsorbed as a water film. The interaction between shale oil as a non-polar molecule and the pore relies on the induced dipole moment induced by polar molecules, which is manifested by weak Coulomb force and van der Waals forces. Since this induced interaction is much weaker than the permanent dipole interaction and hydrogen bonding of the hydrophilic surface, oil molecules fail to adsorb effectively on the surface and mainly exist in the central part

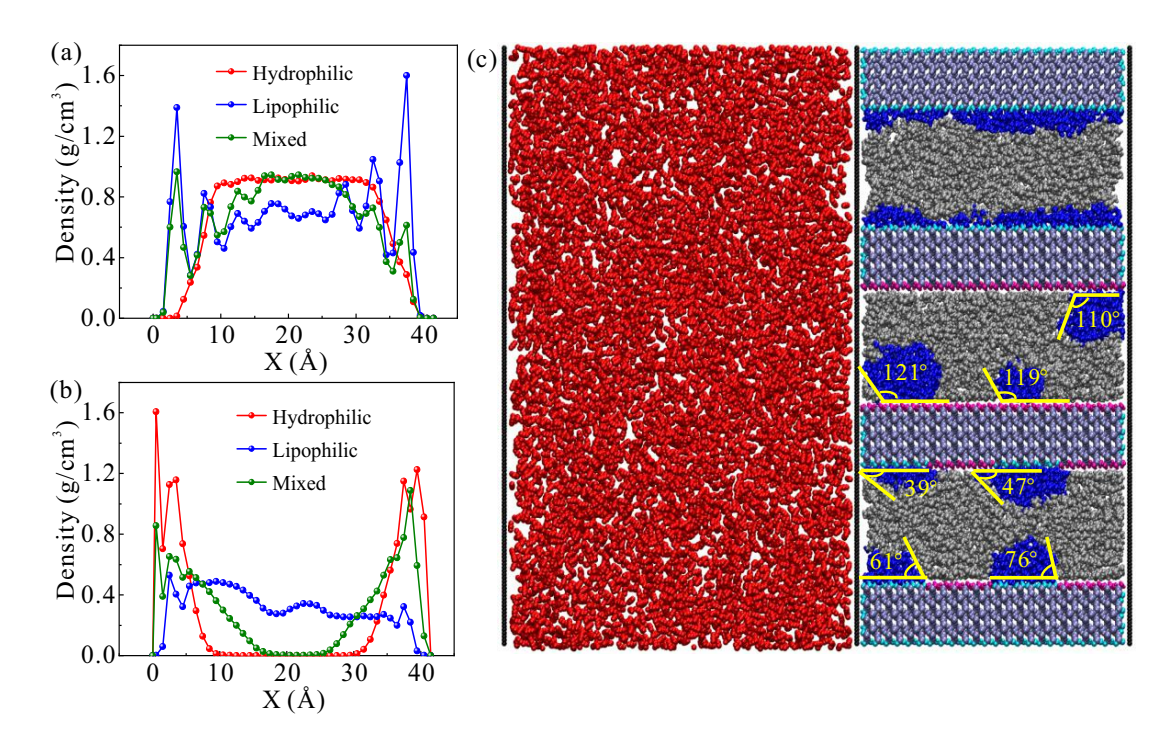


Fig. 3. Density distribution of (a) shale oil, (b) water and (c) molecular dynamics simulation results of the mixed wettability system.

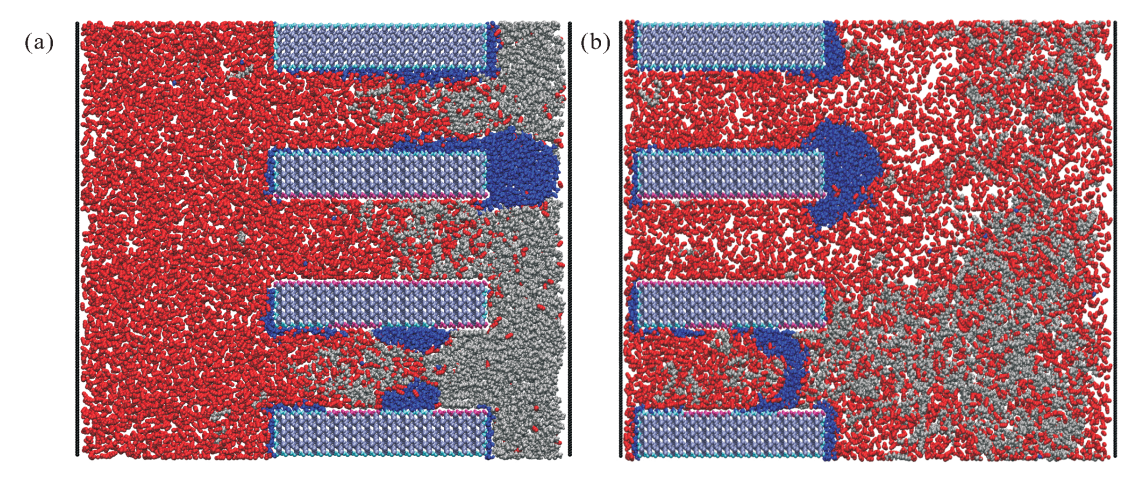
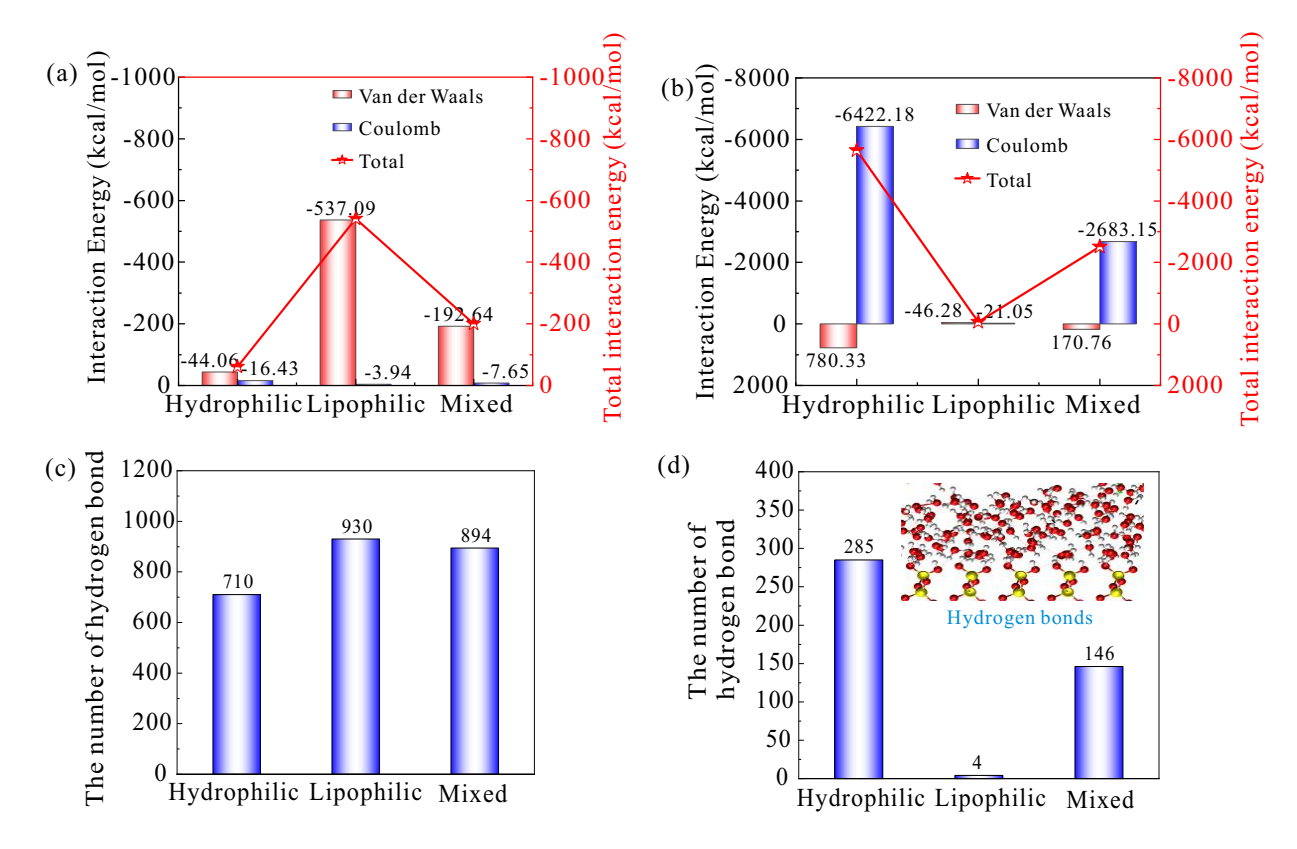


Fig. 4. Displacement process of CO<sub>2</sub>: (a) 1,000 ps and (b) 2,500 ps.

of the pore in a free state. At the beginning of the displacement process, CO<sub>2</sub> can quickly displace the oil molecules with weak attraction to the hydrophilic pore wall, but it can only cause the deformation of the water film. Because oil is weakly attracted to the wall, its molecules encounter less resistance during the CO<sub>2</sub> displacement process and are displaced at a faster rate. However, water molecules adsorb stably as a water film under hydrogen bonding interactions. CO<sub>2</sub> cannot dissolve into water molecules as they are linked by strong hydrogen bonds and can only push the deformation of water film along the direction of the pore outlet.

Inside the lipophilic channel, oil molecules are adsorbed near the surface, while water exist as clusters within the channel. Because shale oil molecules and methyl groups are both non-polar molecules, the instantaneous dipole moments generated by the instantaneous migration of electron clouds within these molecules enable shale oil molecules to be adsorbed on the pore walls through van der Waals forces. Moreover, hydrogen bonds mainly form between highly electronegative atoms. As the electronegativity of oxygen atoms in water molecules is markedly higher than that of carbon atoms in methyl groups, water molecules rely on hydrogen bonding to aggregate into clusters within the channel. After the displacement process begins, almost all of the molecules are effectively mobilized under the action of CO<sub>2</sub> displacement, but the displacement rate is slower than that of the hydrophilic channel system. Since oil molecules are predominantly adsorbed near the lipophilic surface, the adsorbed oil molecules exhibit stronger affinity for the wall and CO<sub>2</sub> needs to overcome greater displacement resistance, resulting in a slower displacement



**Fig. 5**. (a) Interaction energy between oil-surface at 0 ps, (b) interaction energy between water-surface at 0 ps, (c) hydrogen bonds between water molecules at 0 ps and (d) hydrogen bonds between water-surface at 0 ps.

speed.

In the mixed-wetting channel, water molecules adsorb precisely as clusters on the hydrophilic region under the combined action of Coulomb force and hydrogen bonds. Meanwhile, oil is mainly adsorbed on the lipophilic wall region and central regions of the channel through van der Waals forces. After the displacement process begins, water molecules are almost not displaced; instead, the water molecule clusters gradually deform and gather in the hydrophilic regions to form a "water bridge" under the combined effect of displacement pressure difference and intermolecular hydrogen bonds, hindering the subsequent CO<sub>2</sub> displacement process and resulting in some oil persisting in the pore.

#### 3.2 Interphase microscopic mechanism

#### 3.2.1 Selective flow of CO<sub>2</sub>

To further investigate the preferential flow mechanism in a mixed-wettability system, the CO<sub>2</sub> injection volumes in three different-wettability channels were statistically analyzed, as shown in Fig. 6. Within 100 ps, the slope of the curve for the hydrophilic channel is the largest, followed by the mixed-wettability channel, and the lipophilic channel has the smallest slope. The hydrophilic surface exhibits stronger affinity for CO<sub>2</sub> than the lipophilic surface. Therefore, in the initial stage, the count of CO<sub>2</sub> molecules penetrating the hydrophilic channel is the highest, and the number entering the lipophilic channel is the lowest. The entrance of the mixed-wetting

channel is a hydrophilic wall region, but due to the influence of the subsequent lipophilic region, its overall CO<sub>2</sub> injection effect is between the two. Thus, CO<sub>2</sub> preferentially enters the hydrophilic channel, followed by the mixed-wetting channel, and finally the lipophilic channel.

After 100 ps, the CO<sub>2</sub> injection volume curve undergoes a significant transformation. The slopes of the curves for the lipophilic and hydrophilic channels are close, and the slope of the curve for the mixed-wetting channel is significantly lower. This transformation can be attributed to the following points: (1) The weak attraction of the lipophilic surface to water molecules causes water clusters to rapidly leave the channel, not only providing more space for the injection of CO<sub>2</sub> but also disrupting the original arrangement of oil molecules within the channel, making molecular distribution within the channel scarcer and promoting the entry and penetration of  $CO_2$ . (2) The strong attraction of the hydrophilic channel to water molecules prevents the water film from detaching from its surface in the first place. Therefore, the water film occupies the space inside the channel for a long time, restricting the entry of CO<sub>2</sub> into the hydrophilic channel. As a result, the CO<sub>2</sub> can be injected at a similar rate into the hydrophilic and lipophilic channels. (3) The hindrance of "water bridge" in the mixed-wetting channel makes it a limited space blind-end system. The retention of oil molecules further inhibits the entry of CO<sub>2</sub> into the mixed-wetting channel. Therefore, at the end of the displacement process, the number of CO<sub>2</sub> molecules inside the lipophilic and hydrophilic channels is similar, and

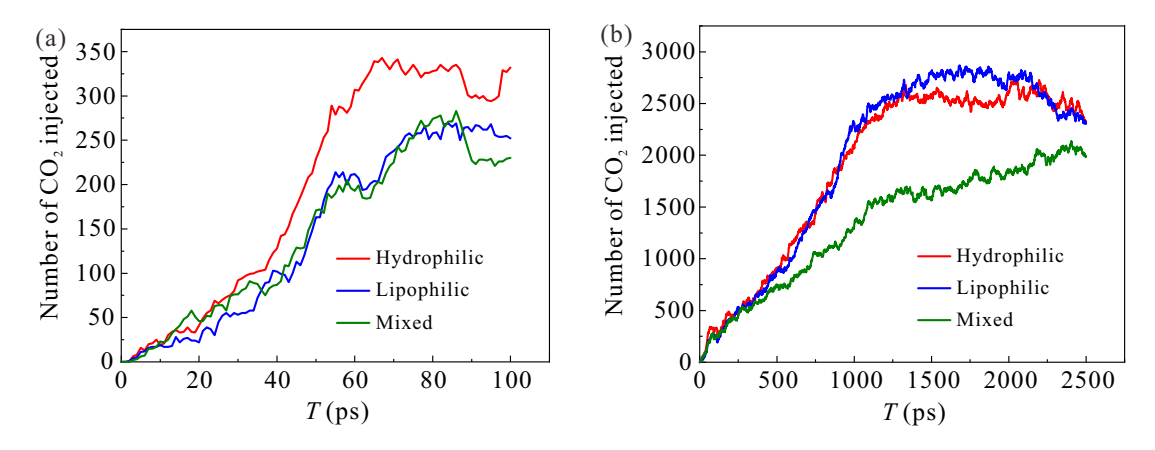


Fig. 6. Injection curves of CO<sub>2</sub> molecules: (a) 100 ps and (b) 2,500 ps.

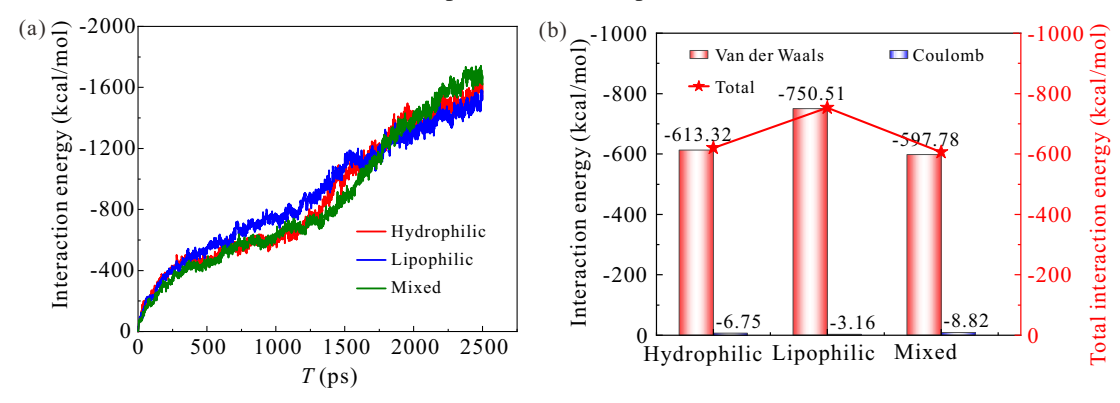


Fig. 7. (a) Oil-CO<sub>2</sub> interaction energy and (b) interaction energy and contribution ratio at 1,000 ps.

much greater than that in the mixed-wetting channel.

#### 3.2.2 Miscibility

The absolute value of miscibility increases with time (Fig. 7(a)), suggesting that  $CO_2$  can effectively disperse the aggregated oil molecules, diminish the dispersion forces among oil molecules, and fully stretch single-chain shale oil molecules, thereby improving the degree of mutual solubility. To clarify the microscopic interaction mechanisms during the miscibility process in channels with different wettability, the non-bonded interaction energy and its contribution ratio between oil-CO<sub>2</sub> molecules in main displacement stage were further quantified, as shown in Fig. 7(b). In the hydrophilic channel, lipophilic channel, and mixed-wetting channel, the van der Waals interactions accounted for 98.91%, 99.58%, and 98.55%, respectively, while the Coulomb interaction accounted for 1.09%, 0.42%, and 1.45% respectively. The continuous vibration of electrons and atomic nuclei inside the molecules during the miscibility process of oil and CO2 leads to instantaneous relative displacement of electron clouds and atomic nuclei, thereby forming instantaneous dipoles. These instantaneous dipoles can induce neighboring molecules to also produce attractive instantaneous dipole interactions through induction, so van der Waals forces exist universally between oil and CO<sub>2</sub> during the miscibility process. In contrast, the generation of Coulomb interaction usually requires molecules to have permanent or induced dipoles. However, CO<sub>2</sub> and oil molecules, as typical non-polar molecules, do not possess permanent dipole moments. Therefore, the Coulomb interaction in the system mainly originates from weak induced dipole interactions, and its energy contribution is only 1.09% to 1.45% of the total non-bonded interaction energy, which can therefore be neglected.

#### 3.2.3 Competitive adsorption

To clarify the competitive adsorption mechanism under mixed wettability and nano-confinement effects, the interaction energy between components in channels with different wettability and the retention ability in the adsorption layer region were statistically analyzed. The greater the interaction energy difference is, the faster the decay speed of the shale oil retention ability curve from 1 to 0, signifying the stronger competitive adsorption ability of CO<sub>2</sub> against oil in the channel, as shown in Figs. 8(a) and 8(b). The difference in the hydrophilic channel is the largest (-585.78 kcal/mol), 2.25 times that of lipophilic channel (-260.75 kcal/mol) and 6.39 times that of mixed-wetting channel (-91.61 kcal/mol). The strong attraction of the hydrophilic channel to CO<sub>2</sub> molecules gives CO<sub>2</sub> an advantage in the competition for oil and CO2 adsorption, resulting in the best competition adsorption effect of oil and CO<sub>2</sub> in the nano-confinement space and the worst retention ability of shale oil molecules. The strong affinity of the lipophilic channel for oil gives rise to abundant adsorbed oil molecules within it, while CO<sub>2</sub> encounters greater resistance in stripping adsorbed oil molecules, resulting in a slower

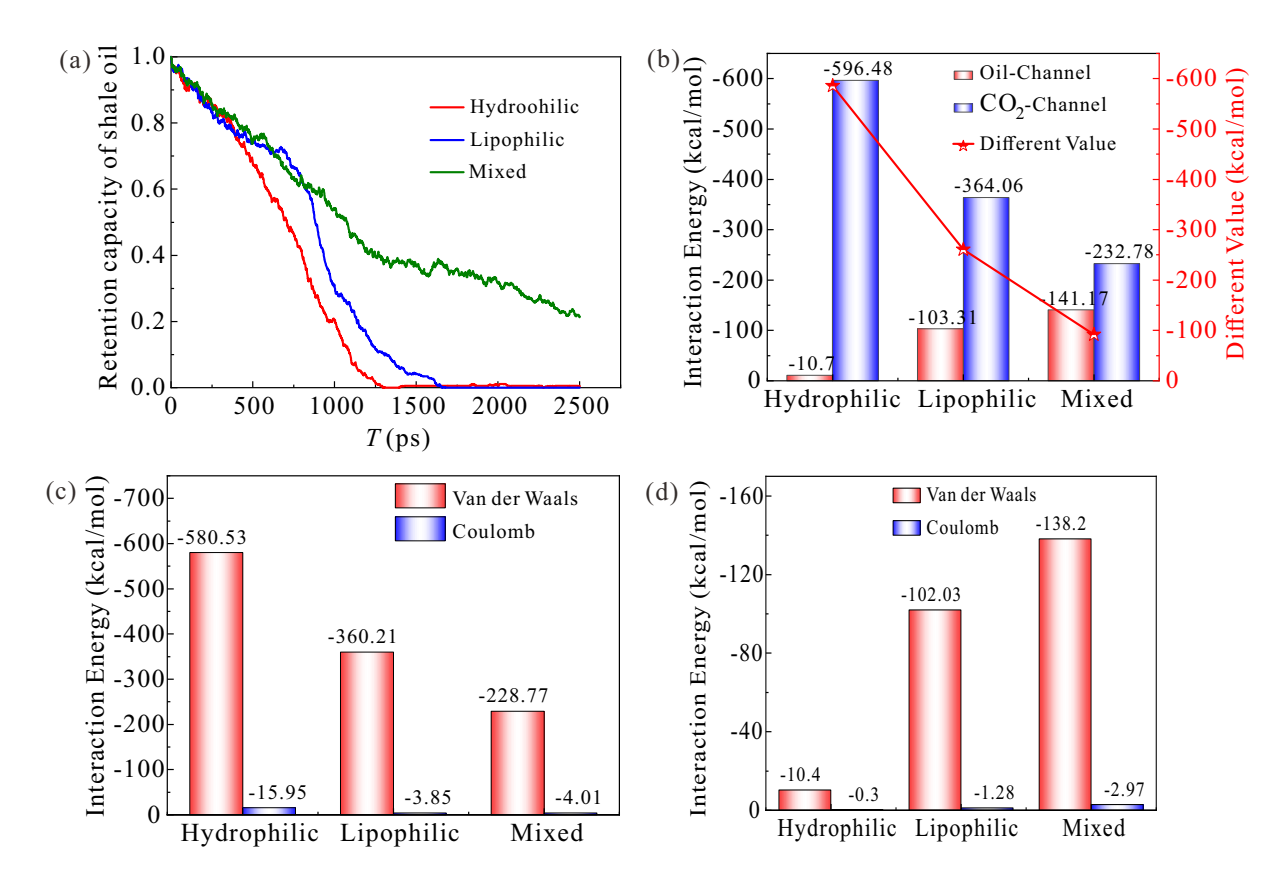


Fig. 8. (a) Shale oil retention ability curve, (b) interaction energy, (c) interaction energy between CO<sub>2</sub>-channel and (d) interaction energy between oil-channel.

stripping and replacement speed. The existence of "water bridges" in the mixed-wetting channel prevents the stripped shale oil molecules from leaving the channel in time, and the curve of shale oil's retention ability cannot be reduced to 0. The competitive adsorption of CO<sub>2</sub> molecules with oil molecules in hydrophilic pores is more advantageous, followed by the lipophilic channel, and then the mixed-wetting channel. Furthermore, the contribution ratios of microscopic forces are shown in Figs. 8(c) and 8(d). In all three channels with different wettability, the interaction is primarily governed by van der Waals forces, while the Coulomb force is relatively weak. Since CO<sub>2</sub> molecules, oil and methyl groups all exhibit nonpolar characteristics, only the hydroxyl groups have significant polarity. Therefore, the interphase microscopic interactions in the system mainly originate from the van der Waals attractive forces produced by instantaneous dipoles within the molecules. By further comparing the contribution rates of Coulomb force between CO<sub>2</sub> molecules and shale oil molecules in channels with different wettability, it was found to be the largest (2.67%, 2.8%) in the hydrophilic channel, followed by the mixed-wetting channel (1.72%, 2.1%), and then the lipophilic channel (1.06%, 1.24%). Hydroxyl groups are polar molecules with significant permanent dipole moment effects due to their fixed charge distribution. When polar molecules approach non-polar molecules, the permanent dipole of the hydroxyl group induces electron rearrangement within the non-polar molecules, leading to the displacement of positive and negative

charges and thus the generation of induced dipole moments. Under the combined action of permanent and induced dipoles, the interphase Coulomb force becomes enhanced.

#### 3.3 Efficiency evaluation

The interphase microscopic interactions in the nanoconfinement space can simultaneously enhance the recovery and help CO<sub>2</sub> to stably adsorb inside the channels, achieving the effect of geological storage. Therefore, the displacement and storage efficiency in nano-confinement space with channels of different wettability were further quantified (Dong et al., 2023a):

$$\eta = \frac{N_t - N_r}{N_t}$$

$$\eta_s = \frac{N_e}{N_t}$$
(6)

$$\eta_s = \frac{\dot{N_e}}{N} \tag{7}$$

where  $\eta$  represents the displacement efficiency;  $N_t$  represents the number of oil in the channel before displacement;  $N_r$ represents the number of oil remaining in the channel after displacement;  $\eta_s$  represents the storage efficiency;  $N_e$  represents the number of oil in the channel.

To clarify the influence of interphase microscopic interaction mechanism on the displacement efficiency, the CO<sub>2</sub> displacement efficiency within channels with different wettability were statistically analyzed, as shown in Figs. 9(a) and 9(b). The results show that the displacement efficiencies for hydro-

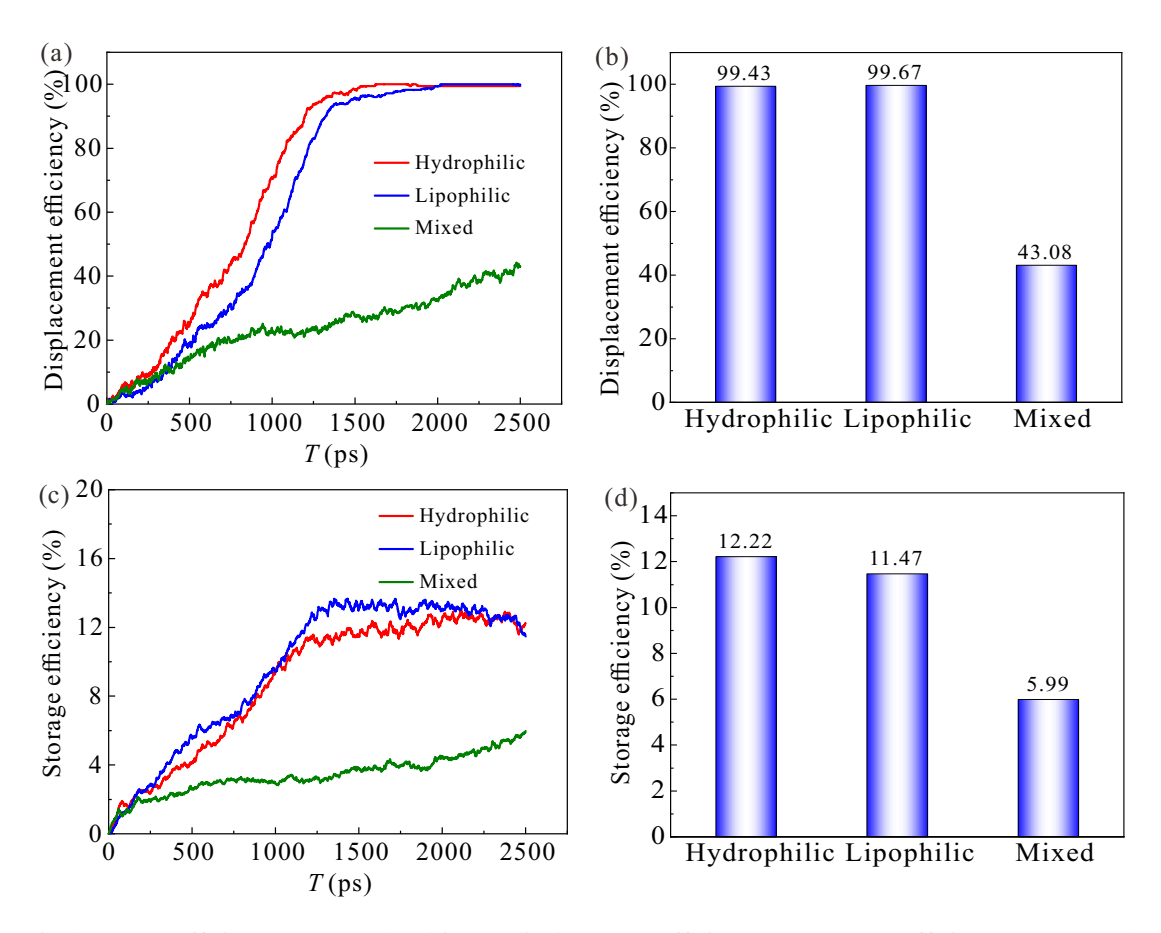


Fig. 9. (a) Displacement efficiency curves, (b) ultimate displacement efficiency, (c) storage efficiency curves and (d) ultimate storage efficiency.

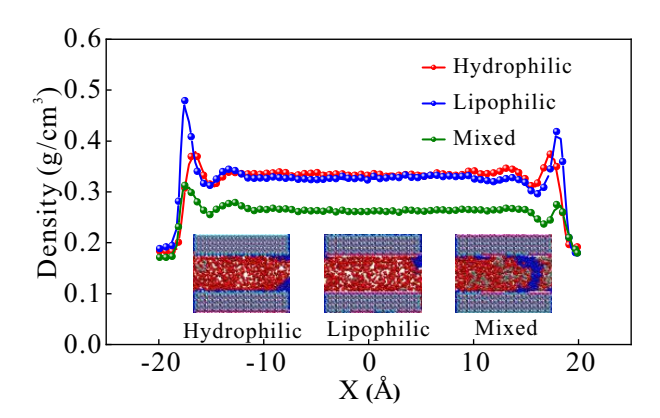


Fig. 10. CO<sub>2</sub> occurrence state and density distribution curves.

philic channel, lipophilic channel, and mixed-wetting channel are 99.43%, 99.67%, and 43.08%, respectively. The miscibility and competitive adsorption effects within these two types of channels are better, allowing more shale oil molecules to be stripped and displaced from the channels, thus resulting in higher  $\rm CO_2$  displacement efficiencies. In contrast, the formation of "water bridges" in mixed-wetting channel severely hinders the  $\rm CO_2$  displacement process, resulting in residual shale oil within the channels and yielding the lowest  $\rm CO_2$  displacement efficiency therein.

To clarify the influence of the interphase microscopic interaction mechanism on the storage efficiency, the  $CO_2$ 

storage efficiency within channels with different wettability were statistically analyzed, as shown in Figs. 9(c) and 9(d). The storage efficiencies for the hydrophilic channel, lipophilic channel, and mixed-wetting channel were 12.22%, 11.47%, and 5.99%, respectively. The water film in the hydrophilic channel gradually detaches from the channel under the longterm displacement effect of CO<sub>2</sub>, providing more space for CO<sub>2</sub> storage, hence the storage efficiency continues to rise. After the displacement process is completed, a thin water film layer still remains near the surface, resulting in a low first adsorption layer of CO<sub>2</sub>. The lipophilic channel has a relatively weak attraction effect on CO2, and the arrangement of its molecules in the central region of the channels is relatively loose. However, since the near-wall region is completely occupied by CO<sub>2</sub>, their first adsorption peak is relatively high (Fig. 10). The "water bridge" in mixed-wetting pore restricts the entry of CO<sub>2</sub> into the pore and also prevents the stripped oil molecules from leaving the pore in time, occupying the storage space of CO<sub>2</sub>. The adsorption layer region is occupied by oil, CO<sub>2</sub> and water phases, resulting in the lowest CO<sub>2</sub> storage efficiency.

#### 4. Conclusions

In this paper, the displacement process of CO<sub>2</sub> within the mixed wettability was simulated by the molecular dynamics method, revealing the complex interphase interaction mecha-

nism within the nanoscale confined space from a microscopic perspective. The main conclusions are as follows:

- Shale oil molecules exist in the form of adsorbed and bulk phases under the action of van der Waals forces; water molecules are adsorbed in the hydrophilic and mixedwetting channels as films and clusters via Coulomb force and hydrogen bonds, and they exist in the lipophilic channel under the action of van der Waals forces.
- 2) CO<sub>2</sub> preferentially enters the hydrophilic channel, followed by the mixed-wetting channel, and finally the lipophilic channel. It not only disperses the aggregated shale oil molecules and reduces the forces between oil molecules but also strips the adsorbed shale oil from the pore walls, achieving miscibility and competitive adsorption effects.
- 3) The instantaneous dipole interactions between non-polar molecules make van der Waals forces the dominant factor in miscibility, while the combined action of permanent dipoles of polar molecules and induced dipoles of non-polar molecules increases the contribution rate of Coulomb force in the competitive adsorption process.
- 4) The displacement efficiencies for the hydrophilic channel, lipophilic channel, and mixed-wetting channel are 99.43%, 99.67%, and 43.08%, respectively, while the storage efficiencies are 12.22%, 11.47%, and 5.99%, respectively. The "water bridge" in the mixed-wetting channel not only limits the ability of CO<sub>2</sub> into the channel but also inhibits the CO<sub>2</sub> displacement and storage effect.

#### Acknowledgements

This research was supported by the National Natural Science Foundation of China (No. 52374035), the Heilongjiang Provincial Natural Science Foundation of China (No. YQ2024E012), the Postdoctoral Projects in Heilongjiang Province (No. LBH-Z20035), and the Qingyan Talent Support Program Project of Daqing Heilongjiang Province (No. DQXY202403).

#### **Conflict of interest**

The authors declare no competing interest.

**Open Access** This article is distributed under the terms and conditions of the Creative Commons Attribution (CC BY-NC-ND) license, which permits unrestricted use, distribution, and reproduction in any medium, provided the original work is properly cited.

#### References

- Alsubaih, S., Sepehrnoori, K., Delshad, M., et al. A Comprehensive review of well integrity challenges and digital twin applications across conventional, unconventional, and storage wells. Energies, 2025, 18(17): 4757.
- Babaei, S., Ghasemzadeh, H., Tesson, S. Methane adsorption of nanocomposite shale in the presence of water: Insights from molecular simulations. Chemical Engineering Journal, 2023, 475: 146196.
- Bao, J., Du, Jia., Zhan, S., et al. A molecular perspective on the microscopic mechanisms of CO<sub>2</sub> injection and water films in fluid transport and enhanced oil recovery.

- Advances in Geo-Energy Research, 2025, 16(3): 288-292.
- Cai, J., Jiao, X., Wang, H., et al. Multiphase fluid-rock interactions and flow behaviors in shale nanopores: A comprehensive review. Earth-Science Reviews, 2024, 257: 104884.
- Chen, K., Zhang, J., Xu, S., et al. Review of carbonated water injection as a promising technology to enhance oil recovery in the petroleum industry: Challenges and prospects. Petroleum Science, 2024, 21(6): 4100-4118.
- Chico, S., Liu, N., Rashid, S., et al. A technical review of CO<sub>2</sub> for enhanced oil recovery in unconventional oil reservoirs. Journal of Petroleum Science and Engineering, 2023, 221: 111185.
- Cui, F., Jin, X., Liu, H., et al. Molecular modeling on Gulong shale oil and wettability of reservoir matrix. Capillarity, 2022, 5(4): 65-74.
- Dong, H., Zhu, Q., Wang, L., et al. Effects of shale pore size and connectivity on scCO<sub>2</sub> enhanced oil recovery: A molecular dynamics simulation investigation. Langmuir, 2023a, 39(17): 6287-6299.
- Dong, X., Xu, W., Liu, H., et al. Molecular insight into the oil displacement mechanism of CO<sub>2</sub> flooding in the nanopores of shale oil reservoir. Petroleum Science, 2023b, 20(6): 3516-3529.
- Goral, J., Panja, P., Deo, M., et al. Confinement effect on porosity and permeability of shales. Scientific Reports, 2020, 10(1): 49.
- Hong, X., Jin, X., Shen, M., et al. Enhancement of oil transport through nanopores via cation exchange in thin brine films at rock-oil interface. Advances in Geo-Energy Research, 2024, 12(1): 22-34.
- Ho, T., Wang, Y. Enhancement of oil flow in shale nanopores by manipulating friction and viscosity. Physical Chemistry Chemical Physics, 2019, 21(24): 12777-12786.
- Humphrey, W., Dalke, A., Schulten, K. VMD: Visual molecular dynamics. Journal of Molecular Graphics, 1996, 14(1): 33-38.
- Janamejaya, C., Ladanyi, B. Hydrogen bond dynamics at the water/hydrocarbon interface. The Journal of Physical Chemistry B, 2009, 113(13): 4045-4053.
- Jiang, W., Lv, W., Jia, N., et al. Study on the effects of wettability and pressure in shale matrix nanopore imbibition during shut-in process by molecular dynamics simulations. Molecules, 2024, 29(5): 1112.
- Lappala, A. The next revolution in computational simulations: Harnessing AI and quantum computing in molecular dynamics. Current Opinion in Structural Biology, 2024, 89: 102919.
- Liu, F., Gao, X., Du, J., et al. Microscopic mechanism of enhancing shale oil recovery through CO<sub>2</sub> flooding-insights from molecular dynamics simulations. Journal of Molecular Liquids, 2024, 410: 125593.
- Masoud, S., Ali, G., Sohrab, Z., et al. Assessment of CO<sub>2</sub>-oil swelling behavior using molecular dynamics simulation: CO<sub>2</sub> utilization and storage implication. Journal of Molecular Liquids, 2023, 379: 121582.
- Mohammed, S., Gadikota, G. The influence of CO2 on the

- structure of confined asphaltenes in calcite nanopores. Fuel, 2019, 236: 769-777.
- Nguyen, D., Phan, T., Hsu, T., et al. Adhesion and surface energy of shale rocks. Colloids and Surfaces A: Physicochemical and Engineering Aspects, 2017, 520: 712-721.
- Perez, F., Devegowda, D. A molecular dynamics study of soaking during enhanced oil recovery in shale organic pores. SPE Journal, 2020, 25(02): 832-841.
- Sanchouli, N., Babaei, S., Kanduc, M., et al. Wetting behavior of kerogen surfaces: Insights from molecular dynamics. Langmuir, 2024, 40(11): 5715-5724.
- Sedghi, M., Piri, M., Goual, L. Atomistic molecular dynamics simulations of crude oil/brine displacement in calcite mesopores. Langmuir, 2016, 32(14): 3375-3384.
- Shi, K., Chen, J., Pang, X., et al. Wettability of different clay mineral surfaces in shale: Implications from molecular dynamics simulations. Petroleum Science, 2023, 20(2): 689-704.
- Thompson, A., Aktulga, H., Berger, R., et al. LAMMPSa flexible simulation tool for particle-based materials modeling at the atomic, meso, and continuum scales. Computer Physics Communications, 2022, 271: 108171.
- Wang, F., Meng, X., Xu, H., et al. Microscopic mechanism of CO<sub>2</sub> imbibition on mixed-wetting surface of shale oil reservoir. Fuel, 2025a, 381: 133592.
- Wang, F., Meng, X., Xu, H., et al. Study on the influence of wettability and displacement pressure on CO<sub>2</sub> storage mechanisms under nano-confinement: Insights from molecular dynamics simulations. Colloids and Surfaces A: Physicochemical and Engineering Aspects, 2025b, 726(1): 137751.
- Wang, H., Kang, Q., Wang, W., et al. Oil-CO<sub>2</sub> phase behavior in nanoporous media: A lattice Boltzmann study. International Communications in Heat and Mass Transfer, 2025, 163: 108738.
- Wang, X., Zeng, J., Kong, X., et al. Controlling effect of shale pore wettability on spontaneous imbibition. Journal of Central South University of Science and Technology,

- 2022, 53(9): 3323-3336.
- Wang, Z., Zhu, J., Li, S. Novel strategy for reducing the minimum miscible pressure in a CO<sub>2</sub>-oil system using nonionic surfactant: Insights from molecular dynamics simulations. Applied Energy, 2023, 352: 121966.
- Wan, Y., Jia, C., Lv W., et al. Recovery mechanisms and formation influencing factors of miscible CO<sub>2</sub> huff-n-puff processes in shale oil reservoirs: A systematic review. Advances in Geo-Energy Research, 2024, 11(2): 88-102.
- William, L., David, S., Julian, T., et al. Development and testing of the OPLS all-atom force field on conformational energetics and properties of organic liquids. Journal of the American Chemical Society, 1996, 118(45): 11225-11236.
- Wu, Z., Sun, Z., Shu, K., et al. Mechanism of shale oil displacement by CO<sub>2</sub> in nanopores: A molecular dynamics simulation study. Advances in Geo-Energy Research, 2024, 11(2): 141-151.
- Xu, H., Wang, F., Liu, Y., et al. Mechanism study on the influence of wettability on CO<sub>2</sub> displacement of shale oil in nanopores. Fuel, 2024, 376: 132695.
- Zhan, S., Su, Y., Jin, Z., et al. Effect of water film on oil flow in quartz nanopores from molecular perspectives. Fuel, 2020, 262: 116560.
- Zhang, L., Cao, C., Wen, S., et al. et al. Thoughts on the development of CO<sub>2</sub>-EGR under the background of carbon peak and carbon neutrality. Natural Gas Industry B, 2023, 10(4): 383-392.
- Zhao, J., Jin, Z., Jin, Z., et al. Origin of authigenic quartz in organic-rich shales of the Wufeng and Longmaxi Formations in the Sichuan Basin, South China: Implications for pore evolution. Journal of Natural Gas Science and Engineering, 2017, 38: 21-38.
- Zhao, Y., Luo, M., Zhang, T., et al. Competitive adsorption of CH<sub>4</sub>/CO<sub>2</sub> in shale nanopores during static and displacement process. Natural Gas Industry B, 2024, 11(3): 239-251.